Cell Cycle 12:9, 1385–1394; May 1, 2013; © 2013 Landes Bioscience

MicroRNA-143 inhibits tumor growth and angiogenesis and sensitizes chemosensitivity to oxaliplatin in colorectal cancers

Xu Qian,[1,†] Jing Yu,[1,2,†] Yu Yin,[1,3] Jun He,[4] Lin Wang,[1] Qi Li,[1] Lou-Qian Zhang,[5] Chong-Yong Li,[1] Zhu-Mei Shi,[6] Qing Xu,[1] Wei Li,[1] Li-Hui Lai,[7] Ling-Zhi Liu[4] and Bing-Hua Jiang[1,4,*]

[1]Department of Pathology; State Key Lab of Reproductive Medicine and Cancer Center; Nanjing Medical University; Nanjing, China; [2]Department of Radiology; the First Affiliated Hospital of Nanjing Medical University; Nanjing, China; [3]Department of Pathology; Anhui Medical University; Hefei, China; [4]Department of Pathology; Anatomy and Cell Biology; Thomas Jefferson University; Philadelphia, PA USA; [5]Department of Oncology; Affiliated Cancer Hospital of Nanjing Medical University; Nanjing, China; [6]Department of Neurosurgery; the First Affiliated Hospital of Nanjing Medical University; Nanjing, China; [7]Institute of Molecular and Chemical Biology; East China Normal University; Shanghai, China

[†]These authors contributed equally to this work.

Keywords: microRNA-143, tumorigenesis, angiogenesis, IGF-IR, chemotherapy

Abbreviations: CAM, chorioallantoic membrane; CRC, colorectal cancer; HIF-1, hypoxia-inducible factor 1; IGF-IR, insulin-like growth factor-1 receptor; miR, microRNA; UTR, untranslated region; VEGF, vascular endothelial growth factor

Colorectal cancer (CRC) is one of the leading cancer-related causes of death in the world. Recently, downregulation of microRNA-143 (miR-143) has been observed in CRC tissues. Here in this study, we found that miR-143 expression was downregulated both in CRC patients' blood samples and tumor specimens. MiR-143 expression levels were strongly correlated with clinical stages and lymph node metastasis. Furthermore, insulin-like growth factor-I receptor (IGF-IR), a known oncogene, was a novel direct target of miR-143, whose expression levels were inversely correlated with miR-143 expression in human CRC specimens. Overexpression of miR-143 inhibited cell proliferation, migration, tumor growth and angiogenesis and increased chemosensitivity to oxaliplatin treatment in an IGF-IR-dependent manner. Taken together, these results revealed that miR-143 levels in human blood and tumor tissues are associated with CRC cancer occurrence, metastasis and drug resistance, and miR-143 levels may be used as a new diagnostic marker and therapeutic target for CRC in the future.

Introduction

CRC is the third leading cause of cancer-related deaths worldwide,[1] characterized with poor prognosis and treatment. It would be important to search for early diagnostic biomarkers to reduce the mortality of CRC.[2,3] MicroRNAs (MiRNAs) are non-protein-coding, 19–22 nucleotide RNAs that regulate expression of a wide variety of genes by targeting their mRNAs, leading to mRNA degradation or inhibition of protein translation.[4,5] MiRNAs are known to play important roles in CRC and other kinds of cancers.[6-8] In particular, studies showed that expression levels of miR-143 are downregulated in many types of cancers, including CRC, but whether its levels are correlated with CRC clinical stages is not known yet. In addition, the roles and mechanisms of miR-143 in regulating angiogenesis, tumorigenesis and drug resistance remain to be elucidated.

The expression profiles of circulating miRNAs in patients' blood are of special interest, because alterations of miRNA signature in circulation are observed in certain cancers and other diseases.[9-14] The levels of specific miRNAs in blood may be used as tumor screening and diagnostic markers as well as predictors of overall patient survival.[15-20] For example, the expression profiles of miR-1, miR-486, miR-30d and miR-499 in serum were served as predictors of overall survival of non-small cell lung cancer.[21] However, so far there is no specific circulating miRNA reported to be associated with CRC development.

IGF-IR is a transmembrane protein that activates a number of downstream signaling pathways including the phosphoinositide 3-kinase (PI3K)/AKT pathway for regulating angiogenesis and tumorigenesis.[22] Recent studies have identified some miRNAs post-transcriptionally regulating IGF-IR, such as miR-145, miR-375 and miR-7.[23-25] IGF-IR also plays important roles in regulating CRC resistance to oxaliplatin, one of the standard first-line treatments of CRC.[26,27] However, the mechanism underlying IGF-IR-mediated drug resistance remains unclear.

*Correspondence to: Bing-Hua Jiang; Email: binghjiang@yahoo.com
Submitted: 12/14/12; Revised: 03/26/13; Accepted: 03/27/13
http://dx.doi.org/10.4161/cc.24477

In this study, we aim to address the following questions: (1) Whether miR-143 expression is detectable in circulating blood, which may be associated with cancer development; (2) What is the role of miR-143 in tumor growth and angiogenesis; (3) What is/are functional target(s) of miR-143 involved in tumor growth and angiogenesis; and (4) What role of miR-143 and underlying mechanisms in CRC resistance to oxaliplatin treatment.

Results

Downregulation of miR-143 expression in blood samples and tumor tissues of human CRC patients. To determine the expression level of miR-143 in circulating blood samples, qRT-PCR analysis was performed in plasma samples from 41 CRC patients and 10 healthy subjects. The results showed that miR-143 expression was detectable in both cancer patients' and healthy subjects' specimens. Interestingly, miR-143 expression levels were significantly decreased in the plasma samples of CRC patients when compared with the normal subjects (**Fig. 1A**), suggesting miR-143 expression can be a potential biomarker as a noninvasive diagnostic tool. We also tested the expression levels of miR-143 in 62 pairs of cancer tumor specimens and adjacent normal tissues and found that miR-143 expression levels in tumor tissues were significantly lower than those in adjacent normal ones (**Fig. 1B**). We also compared the miR-143 expression levels among different stages. We found that the miRNA expression levels in cancer tissues were correlated with the stages of CRC patients. The late stages C+D showed even lower miR-143 expression levels than those in early stages A and B (**Fig. 1C** and **Table 1**). In addition, miR-143 levels were markedly lower in the patients with lymph node metastasis than those in the patients without lymph node metastasis (**Fig. 1D**), which was consistent with the above result, since lymph node metastasis commonly occurs in Duke's stages C and D, but not in Duke's stages A and B. Taken together, the low expression levels of circulating miR-143 in blood samples of CRC patients and tumor tissues were closely related with stages and metastasis, indicating that circulating miR-143 levels may be used as a potential new biomarker for the diagnosis of CRC.

MiR-143 overexpression inhibits cell proliferation and migration, and suppresses expression of HIF-1α and VEGF. To test the direct role of miR-143 in CRC cells, we established stable cell lines by infecting SW1116 cells with lentivirus carrying miR-143 or the negative control precursor (miR-NC) followed by puromycin selection. High levels of miR-143 expression were confirmed in the SW1116/miR-143 stable cell line (**Fig. S1A**). Cell viability assay indicated that overexpressing miR-143 significantly reduced cell growth rate 48 h after seeding (**Fig. 2A**). Forced expression of miR-143 also markedly reduced the wound-healing rate in cancer cells (**Fig. 2B**). To test the involvement of downstream signaling molecules, we showed that miR-143 expression inactivated AKT and downregulated protein levels of HIF-1α, which is a major regulator of VEGF expression at transcriptional level (**Fig. S1B**). qRT-PCR assay showed a significant decrease of VEGF mRNA levels in SW1116/miR-143 cells by almost 70% when compared with those of the negative control (**Fig. S1C**). Consistent with this result, secreted VEGF protein levels were decreased by 45% in the culture medium of SW1116 cells overexpressing miR-143 cells (**Fig. S1D**). These findings indicate that miR-143 functions as suppressor of cell proliferation and migration in CRC cells.

Table 1. Comparison of clinical patothologic factors and normalized expression levels of miR-143 in 62 pairs of CRC tissues

Colorectal cancer	n	Normalized expression of miR-143[a]
Duke's stage		
A	11	0.5174 (0.3559–0.7727)
B	23	0.5361 (0.3495–0.6908)
C + D	28	0.3879 (0.2074–0.5182)
p value		0.0188
Lymph node		
Negative	34	0.536 (0.3551–0.6920)
Positive	28	0.399 (0.1962–0.5225)
p value		0.0065

"a" indicates median values of normalized expression levels of miR-143 with 25th-75th percentile in parenthesis.

IGF-IR is a direct target of miR-143. To determine the functional target of miR-143, we searched for putative targets of miR-143 by using the Targetsearch algorithm developed by ourselves, and found a putative miR-143 binding site in 3'-UTR of IGF-IR. This binding site was totally conserved in at least six kinds of species including human, rhesus monkey, mouse, rat, dog and cow (**Table S1**). To experimentally validate whether miR-143 directly targets IGF-IR, we cloned the 3'-UTR region of IGF-IR with wild type or mutant miR-143 binding sites, respectively, into pMIR-REPORTER vector as indicated in **Figure 3A**. Forced expression of miR-143 markedly decreased wild type reporter activities by almost 40%, whereas the mutant reporter luciferase activities weren't affected, suggesting that the predicted binding sites were the binding regions of miR-143 within IGF-IR 3'-UTR (**Fig. 3B**). Western blotting showed that miR-143 overexpression was sufficient to inhibit IGF-IR protein expression (**Fig. 3C and D**). In order to investigate the relationship between expressions of miR-143 and IGF-IR in human CRC specimens, we analyzed the levels of IGF-IR expression in 62 pairs of CRC samples by immunohistochemistry (IHC). The relative expression levels of IGF-IR were analyzed by two experienced pathologists in a blind manner and marked as final IHC scores: 0 (negative), + (weak), ++ (moderate) and +++ (strong). When the levels of miR-143 were much lower, the intensities of IGF-IR were much higher (**Fig.3E**). Scatter plot analysis showed an inverse correlation between miR-143 expression levels and IHC scores of IGF-IR signals (**Fig. 3F**). These results demonstrated that miR-143 directly inhibited IGF-IR expression by directly targeting its 3'-UTR region, and miR-143 expression levels were inversely correlated with IGF-IR levels in CRC tissues.

MiR-143 inhibits tumor angiogenesis and tumor growth. We employed the chorioallantoic membrane (CAM) system to test the effects of miR-143 on angiogenesis. As shown in

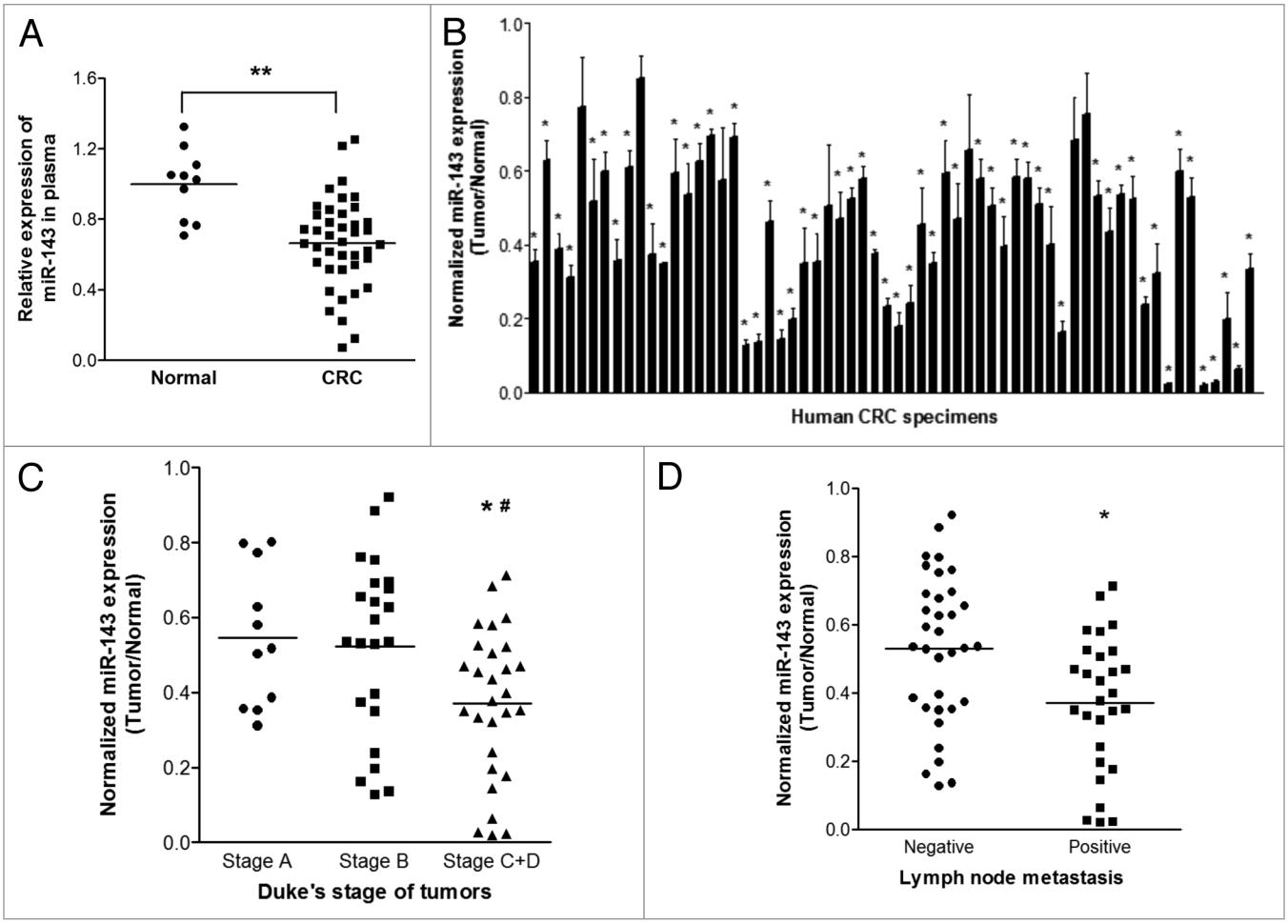

Figure 1. MiR-143 expression levels are downregulated in blood samples and cancer tissues and correlated with CRC clinical stages. (**A**) The relative expression levels of miR-143 in plasma of CRC patients were detected and normalized to those of the spiked-in control cel-miR-39. **p < 0.001 indicates significant difference comparing miR-143 expression levels in the plasma from CRC patients and from healthy subjects. (**B**) Expression levels of miR-143 in 62 pairs of CRC tumor tissues and adjacent normal specimens were analyzed by stem-loop qRT-PCR and normalized to the levels of U6. The fold changes were obtained by the ratio of miR-143 abundance in cancer tissues to that in the adjacent normal tissues. *p < 0.05 indicates significant difference comparing miR-143 expression in tumor tissues with adjacent normal tissues. (**C**) Relative expression levels of miR-143 in different stages of cancer tissues. *p < 0.05 indicates significant difference comparing miR-143 expression in Duke's stage C+D with stage A, while #p < 0.05 comparing miR-143 expression in Duke's stage C+D with stage B. (**D**) Relative expression levels of miR-143 in different types of lymph node metastasis. *p < 0.05 comparing miR-143 expression in positive lymph node metastasis with negative one.

Figure 4A, forced expression of miR-143 in SW1116 cells significantly suppressed the angiogenesis responses by 40% when compared with the negative control. To test the effect of miR-143 on tumor growth, SW1116 cells overexpressing miR-143 or miR-NC were subcutaneously injected into posterior flank of nude mice (n = 6). Xenograft tumor volumes were measured every 2 d when they were palpable. On day 16 after implantation, tumors from cells overexpressing miR-143 were significantly smaller than those from control cells (**Fig. 4C**). Nude mice were sacrificed on day 24 after implantation, and xenografts were collected and weighed. Representative xenograft tumors were shown in **Figure 4B**. When compared with controls, the average tumor weights from the miR-143-overexpression group were markedly reduced by 80% (**Fig. 4D**). Total proteins from representative tumor samples were analyzed by western blotting, and it was determined that miR-143 suppressed its target IGF-IR expression in vivo (**Fig. 4E**). It was also confirmed that VEGF expression in xenograft tumors were significantly decreased by miR-143 by 30% (**Fig. 4F**).

MiR-143 inhibits cell proliferation and sensitizes CRC cells to oxaliplatin treatment through IGF-IR. To investigate whether IGF-IR, the target gene of miR-143, was involved in miR-143-regulated cell proliferation, we overexpressed IGF-IR protein levels in SW1116/miR-143 cells by infecting cells with lentivirus carrying IGF-IR (**Fig. S2A**), and restoration of IGF-IR also rescued AKT activity and VEGF expression suppressed by miR-143 (**Figs. S2A and B**). As expected, overexpression of IGF-IR reversed miR-143-mediated suppression of cell growth (**Fig. 5A**). To explore the role of miR-143 in chemotherapy, we treated CRC cells with different concentrations of oxaliplatin, a leading chemo-drug used for treatment of CRC. Cell viability was determined after 72 h treatments. As shown in **Figure 5B**,

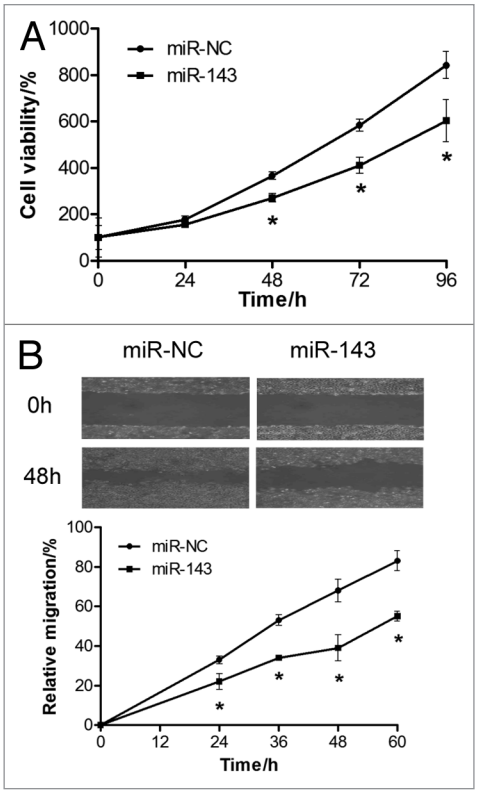

Figure 2. MiR-143 overexpression suppresses proliferation and migration of SW1116 cells. (**A**) Cell viability was evaluated. Results were means ± SE from three independent experiments performed in sextuple. (**B**) SW1116 cells stably overexpressing miR-143 or miR-control were cultured to 90% confluence. A sterile 200 μl pipette tip was used to scratch the cells to form a wound. The wound gaps were photographed (top) and measured (bottom).

overexpression of miR-143 in CRC cells significantly increased chemosensitivity to oxaliplatin treatment, while IGF-IR overexpression reversed the chemosensitivity process. Cell growth rate was tremendously inhibited by miR-143 and restored by IGF-IR overexpression with oxaliplatin treatment (**Fig. S2C**). In order to explore whether miR-143 plays a role in cell apoptosis that is relevant to oxaliplatin treatment, cell apoptosis rates in the presence of oxaliplatin (4 μM) were assayed by FACS analysis at indicated times. Overexpression of miR-143 alone didn't affect cell apoptosis; nevertheless, when it combined with oxaliplatin treatment, cell apoptosis was significantly induced (**Fig. 5C**). More intriguingly, IGF-IR overexpression reversed the effect induced by miR-143. Western blotting analysis also showed that caspase-3, a key executor of cell apoptosis, was involved in the apoptosis process. Caspase-3 remained inactive in cells with miR-143 overexpression alone. But when cells were treated with oxaliplatin along with miR-143 overexpression, caspase-3 was activated, whereas IGF-IR overexpression reversed the activation of caspase cleavage (**Fig. 5D**). These results indicated that miR-143 induced CRC chemo-sensitivity to oxaliplatin treatment in an IGF-IR-dependent manner. To our knowledge, this finding is the first time to show that miR-143 increases CRC chemosensitivity to oxaliplatin treatment through caspase-3.

Discussion

Since *lin-4* was first discovered by Ambros and colleagues,[28] miRNAs have been among one of the most actively researched fields due to their important functions in gene regulation.[29-31] Recent studies showed that miRNAs can be secreted into the blood system by normal cells and/or tumor cells, and are found to be stable in serum or plasma.[9,10,13] In this study, we analyzed the expression levels of miR-143 in plasma from CRC patients and healthy subjects and, interestingly, found that circulating miR-143 expression levels were significantly lower in CRC patients than in healthy subjects. Here, we demonstrated that miR-143 expression was detectable in human blood, with expression levels correlating with the downregulation of miR-143 levels in human CRC tissues. Moreover, we also found that the downregulation of miR-143 expression was associated with later clinical cancer stages and lymph node metastasis in CRCs. These results strongly suggested that circulating miR-143 expression levels have clinical implications, which may be used as a new biomarker for CRCs.

MiR-143 may play a potential role as a tumor suppressor in many kinds of cancers, including CRC.[32-34] Angiogenesis plays vital roles in tumor growth, which requires well-orchestrated molecular events during this process. Here, we reported that miR-143 functions as an anti-angiogenic regulator in CRC tumor growth. Overexpression of miR-143 in CRC cells led to reduced amount of microvessels in a CAM model and impaired tumor growth in a xenograft model in nude mice. Further studies indicated that miR-143 inactivated AKT and inhibited its downstream modulators, HIF-1α and VEGF, key regulators in angiogenesis and tumorigenesis.[35,36]

IGF-IR is a key regulator of tumor development which plays vital roles in regulating cell proliferation, differentiation and survival.[37,38] We and others' labs have demonstrated that IGF-IR promotes angiogenesis and tumor growth through the PI3K/AKT downstream pathway.[39-41] Moreover, we found that IGF-IR also functioned in the process of chemoresistance to oxaliplatin, a first-line regimen for CRC treatment.[42-44] We identified IGF-IR as a novel direct target of miR-143 and as a very important linker in the miR-143-mediated tumor suppression events. Moreover, we found that miR-143 overexpression increased chemosensitivity of cancer cells to oxaliplatin treatment in vitro, indicated by decreased cell viability and increased cell apoptosis. Re-expression of IGF-IR reversed the miR-143-mediated effect in drug resistance of CRC cells, suggesting that IGF-IR played central roles in miR-143-induced chemosentivity to oxaliplatin treatment. Further experiments are needed to deeply elucidate how IGF-IR is involved in miR-143-induced chemosensitivity.

In summary, our present investigation suggests that miR-143 functions as a tumor suppressor by negatively regulating IGF-IR expression via specifically targeting its 3'-UTR region. In human CRC tissues, miR-143 levels are inversely related with the protein levels of IGF-IR. MiR-143 impairs tumor growth and angiogenesis through the PI3K/AKT/HIF-1/VEGF pathway. Interestingly, we demonstrate that miR-143 sensitizes oxaliplatin treatment in an IGF-IR-dependent manner. We also

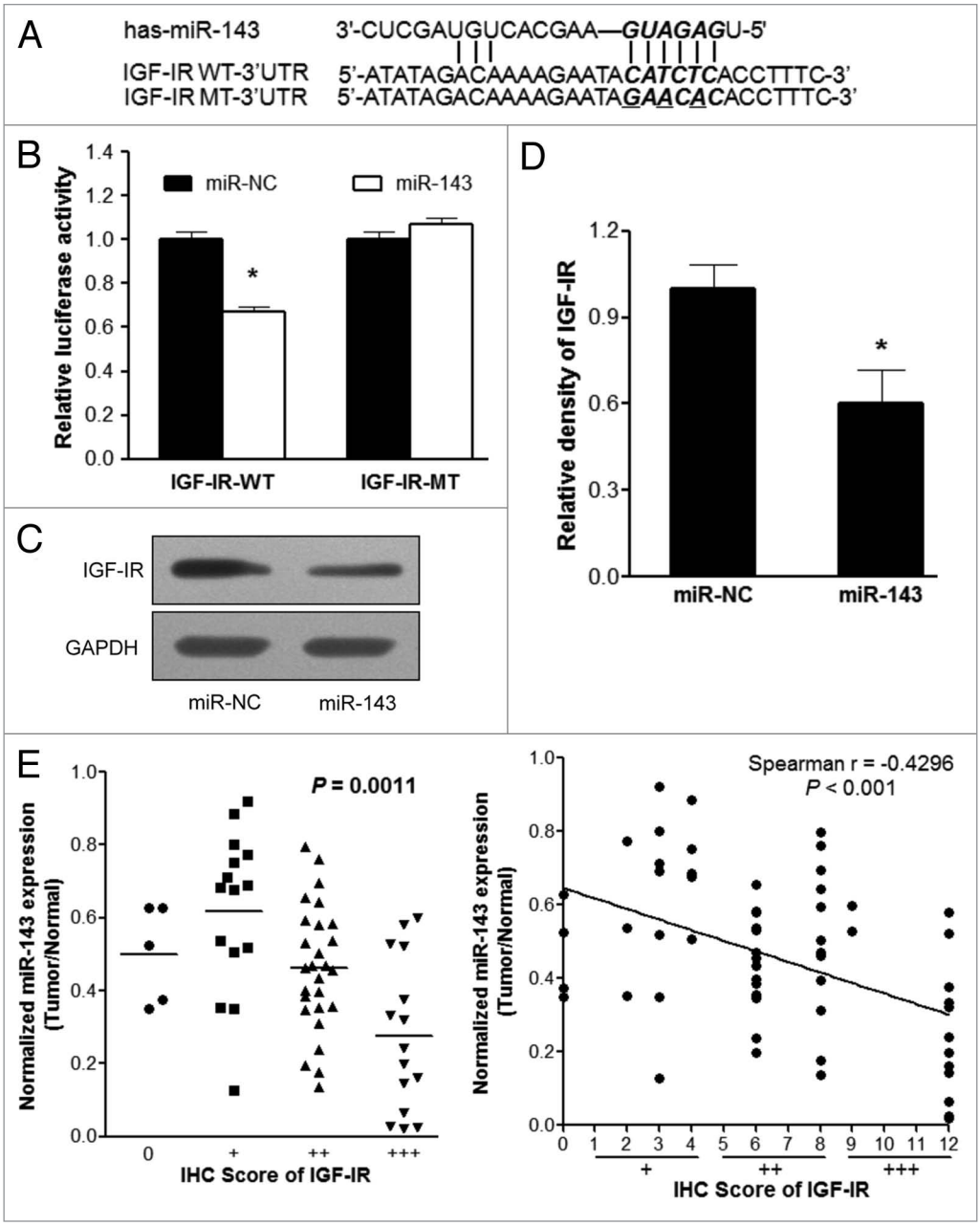

Figure 3. IGF-IR is a direct target of miR-143. (**A**) Putative seed-matching sites (in bold and italic) or mutant sites (underlined) between miR-143 and 3'-UTR of IGF-IR. (**B**) Luciferase activities of reporter constructs containing wild-type (WT) or mutant (MT) 3'-UTR of IGF-IR were assayed and normalized to those of renilla activities (internal control). Data were presented as means ± SE from three independent experiments with triple replicates per experiment. (**C and D**) Total proteins were subjected to western blotting and detected for IGF-IR expression levels. Relative densities of protein expression signals were calculated and normalized to GAPDH protein levels from three separate experiments. Data were means ± SE. (**E**) The correlation analysis was performed between IGF-IR protein levels and miR-143 expression levels in CRC tissues. The IHC scores were used to describe protein levels of IGF-IR in tumor tissues, which were evaluated by experienced pathologists in a blind manner. (**F**) Linear regression curves of miR-143 expression and IGF-IR protein levels. *p < 0.05 comparing miR-143 with scrambled miRNA control (miR-NC).

demonstrated that miR-143 expression is not only decreased in human CRC specimens associated with clinical features, but also is downregulated in patients' circulating bloods. Taken together, these findings suggest that miR-143 may be a useful biomarker for CRCs and provide new information for using miR-143/IGF-IR-based therapeutic strategies for CRC treatments in the future.

Materials and Methods

Clinical specimens. Paired human CRC specimens and matched normal adjacent tissue samples were collected from patients undergoing standard surgical procedures in the First Affiliated Hospital of Anhui Medical University, with the informed consent of the patients. Parts of tissue samples were immediately

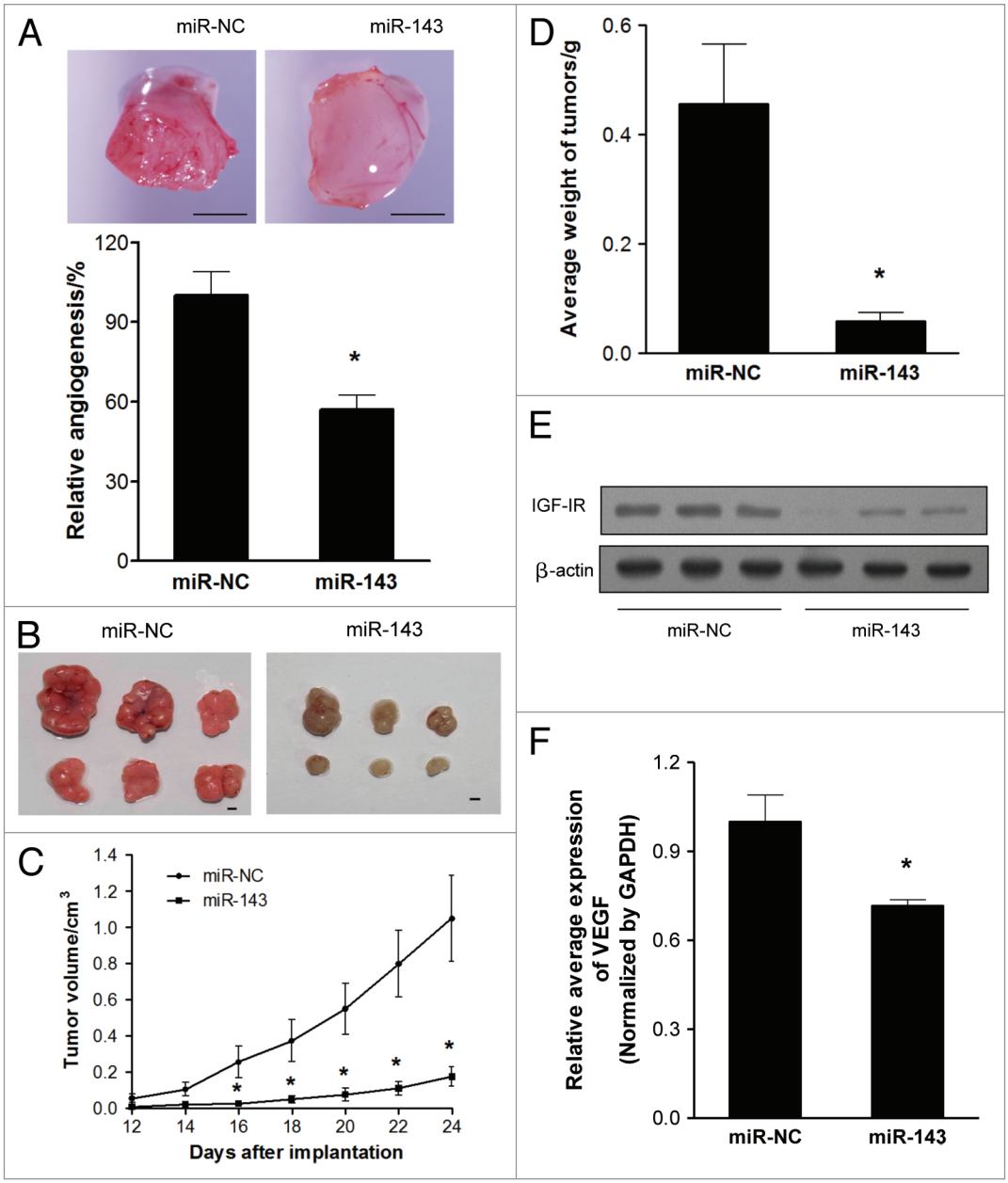

Figure 4. MiR-143 inhibits angiogenesis and tumorigenesis in vivo. (**A**) Angiogenesis assay by chorioallantoic membrane (CAM) model as described in "Materials and Methods." Top: Representative CAM plugs. Bar = 2 mm. Bottom: The branches of blood vessels, which were counted as the index of angiogenesis was obtained from the CAMs of 8–10 embryos per treatment 96 h after implantation. The data represented as mean ± SE of blood vessel numbers were normalized to those of the control. (**B**) Tumor growth assay in nude mice (n = 6). Representative pictures of xenograft tumors are shown. Bar = 2 mm. (**C**) Tumor growth curve upon implantation. (**D**) The average weights of xenograft tumors. Data were means ± SE. (**E**) Protein levels of IGF-IR in xenograft tumors. (**F**) qRT-PCR analysis of VEGF mRNA levels in xenograft tumors. Data were presented as means ± SE *p < 0.05 indicates significant difference comparing miR-143 treatment and miR-NC (control).

snap-frozen in liquid nitrogen, and parts were fixed in formalin for histological examination. All samples were histologically classified and graded according to Duke's stage by clinical pathologist. No information regulated by HIPPA was included in the study. The experiment protocols were approved by the Institutional Review Committees of Anhui Medical University and Nanjing Medical University.

Plasma collection and plasma RNA extraction. Whole human bloods were collected from Anhui Medical University, Hefei, with the consent of patients and healthy subjects. The protocols were approved by Institutional Review Committees of Anhui Medical University and Nanjing Medical University. Plasma was isolated from whole blood by centrifuging at 1,400 rpm for 10 min and was stored at −80°C refrigerator. The plasma RNAs were extracted following a similar procedure as described previously.[45] In brief, a volume of 300 μL of blood and 900 μL of TRIZol (Invitrogen) were thoroughly mixed and followed by adding manual synthetic *C. elegans* miR-39 (cel-miR-39) to final

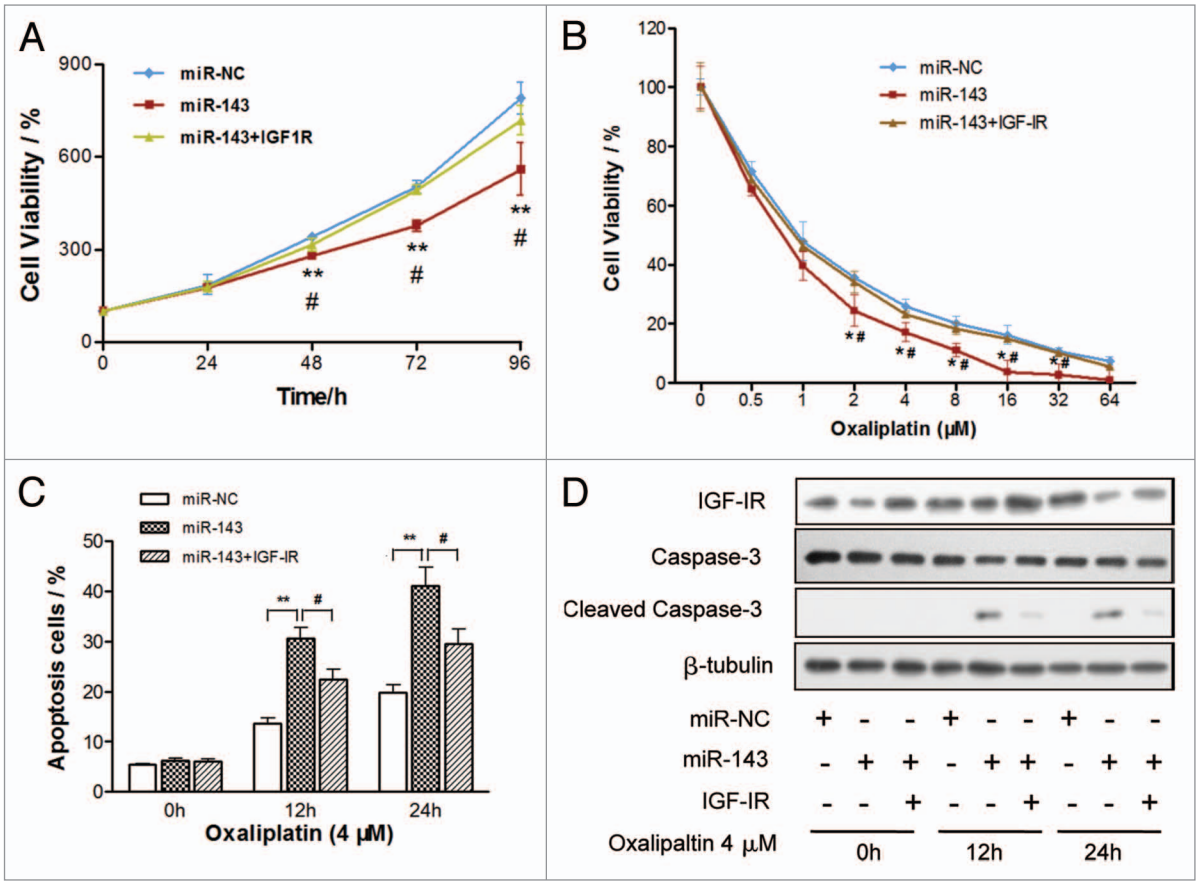

Figure 5. MiR-143 increases chemosensitivity of CRC cells to oxaliplatin treatment through IGF-IR. (**A and B**) Cell viability was evaluated in cells stably expressing scrambled miRNA control (miR-NC), miR-143 or miR-143 + IGF-IR, respectively, with (**A**) or without (**B**) the oxaliplatin treatments at different doses. Data were means ± SE. (**C and D**) Cells stably expressing miR-NC, miR-143 or miR-143 + IGF-IR were treated with 4 μM of oxaliplatin at indicated time points and subjected to apoptosis analysis by flow cytometry (**C**) and western blotting (**D**). Data were means ± SE **$p < 0.001$ indicated significance between group of miR-143 and control group miR-NC, while #$p < 0.05$ represented significance between group of miR-143 and group of miR-143 + IGF-IR.

concentration of 10^{-5} nM as spiked-in control. Total RNAs were extracted using Trizol solution according to the manufacturer's instructions, and eluted in 30 μL DEPC-treated water. Aliquots of RNAs (5 μL) were used to perform reverse transcription reactions as templates and analyzed by qRT-PCR.

Cell culture. Human CRC cell line SW1116 and derived stable cell lines were cultured in RPMI 1640 medium, and HEK293T cells were cultured in DMEM medium supplemented with 10% fetal bovine serum, 100 units/ml penicillin and 100 μg/ml streptomycin in a 37°C incubator containing 5% CO_2.

Lentiviral packaging and stable cell line establishment. To stably overexpress miR-143 in CRC cells, the lentiviral packaging kit was used (Thermo Fisher Scientific). Lentivirus carrying miR-143 or negative control (miR-NC) was packaged following the manufacturer's manual. Red fluorescent protein (RFP) gene was inserted into the packaging system and co-expressed with miRNAs. Lentivirus was packaged in HEK293T cells and secreted into the medium. SW1116 cells were infected by lentivirus carrying miR-143 or miR-NC with the presence of polybrene (Sigma-Aldrich) and selected by puromycin (Sigma-Aldrich) for 2 wk to obtain SW1116/miR-143 and SW1116/miR-NC stable cell lines. To overexpress IGF-IR in CRC cells, lentivrius carrying IGF-IR ORF cDNA (GeneCopoeia) were packaged and used to infect cells as instructed by manufacturer's manual.

Cell viability assay. One thousand cells per well were seeded and cultured in 96-well plates. Cell viability was assayed using a CCK8 kit (Dojindo Laboratories) according to the manufacturer's instruction at indicated time points. All results were obtained from three separate experiments with six replicates per experiment.

Wound healing assay. Cells were cultured until reached 90% confluence in 6-well plates. Cell layers were scratched using a 200 μL tip to form wounded gaps, washed with PBS twice and cultured. The wounded gaps were photographed at different time points and analyzed by measuring the distance of migrating cells from five different areas for each wound.

In vitro chemosensitivity array. Cancer cells were seeded at a density of 4,000 cells per well in a 96-well plate overnight. Freshly prepared oxaliplatin (Sigma-Aldrich) was added with the final concentration ranging from 1 to 64 μM. Seventy-two hours later, cell viability was assayed by CCK8 kit.

Apoptosis assay. Apoptosis were measured by flow cytometry as described before.[46] Briefly, cells were trypsined and labeled with Alexa Fluor 647 Annexin V (Biolegend) and 7-AAD (BD PharMingen), and subjected to FACS analysis. Cells were considered apoptotic when they were annexin V-positive and 7-AAD-negative.

Transfections and dual-luciferase reporter assay. 3'-UTR of IGF-IR was amplified by PCR using Pfu DNA polymerase from cDNA library prepared from SW1116 cells, and inserted into pMIR-REPORTER vector (Ambion). Primers used for wild type and mutant reporter constructs were listed in **Table S2**. Wild type and mutant constructs were validated by DNA sequencing. SW1116 cells were seeded in 24-well plates and co-transfected with 0.3 μg of luciferase reporter plasmids, 0.1 μg of Renilla luciferase reporter (internal control) and equal amounts (30 nM) of pre-miR-143 or pre-miR-NC (Ambion) using Lipofectamine 2000 (Invitrogen). Firefly and Renilla luciferase activities were measured 24 h after transfection using a dual luciferase assay kit (Promega). Experiments were repeated three times with three replicates each.

RNA isolation and quantitative real-time PCR (qRT-PCR) analysis. Total RNAs were extracted from cultured cells or human tissue specimens using TRIzol reagent according to the manufacturer's instruction. To quantify the mRNA levels of VEGF, RNAs were transcribed using PrimeScript RT Reagent Kit and oligo dT primer (Takara). To measure miR-143 expression levels, RNAs were transcribed by stem-loop RT primer using PrimeScript RT Reagent Kit (Takara) as previously described.[47,48] qRT-PCR was performed using SYBR Premix DimerEraser (Takara) on a 7900HT system. GAPDH or U6 levels were used as an internal control, respectively. Primers were listed in **Table S2**.

Protein extraction and western blotting. Cells or tissues were harvested and lysed on ice for 30 min in RIPA buffer (Beyotime) supplemented with 1 mM phenylmethylsulfonyl fluoride (PMSF). Lysates were subjected to western blotting assay, as described before,[49] and detected with antibodies against IGF-IR, phospho-AKT (Ser-473), total AKT, β-tubulin (Cell Signaling Technology), HIF-1α, HIF-1β (BD Biosciences), GAPDH (Santa Cruz Biotechnology) or β-actin (Sigma-Aldrich).

Chorioallantoic membrane (CAM) angiogenesis assay. Fertilized chicken eggs were incubated at 37°C with 70% humidity for 8 d. An artificial air sac was created as we previously described.[50] Cells were suspended in serum-free medium and mixed with equal volume of growth factor-reduced Matrigel (BD Biosciences). Aliquots (3×10^6, 60 μL) of the mixture were applied onto the CAM of 9-d-old embryos. The plugs were trimmed out and photographed 4 d after the implantation, and the number of blood vessels was obtained by counting the branching of the blood vessels.

Immunohistochemistry (IHC). Formalin-fixed, paraffin-embedded tissues of 62 pairs of human CRC specimens were sectioned at 5 μm and incubated with antibodies against IGF-IR (Cell Signaling Technology). The assessment of IHC signals was performed by two experienced pathologists in a blind manner. Five high-power fields (200×) of every sample were randomly selected. Percentages of positive tumor cells were categorized into five semi-quantitative classes: 0 (≤ 5% positive cells), 1 (6–25% positive cells), 2 (26–50% positive cells), 3 (51–75% positive cells) and 4 (> 76% positive cells). Intensity of staining was also semi-quantitatively determined on a scale of 0–3 as follows: 0 (negative), 1 (weakly positive), 2 (moderately positive) and 3 (strongly positive). Multiplication of percentage scores and intensity of staining gave the final IHC score: 0 (negative), + (1–4), ++ (5–8) and +++ (9–12) as previously described.[51]

Xenograft tumor model in nude mice. For tumor growth assay, male nude mice [BALB/cA-nu (nu/nu), 6-wk-old] were purchased from SLAC Animal Center and maintained in special pathogen-free (SPF) conditions. Animal protocols were approved by the Animal Welfare Committee of Nanjing Medical University. Aliquots of cells (4×10^6) were suspended in 150 μl of FBS-free RPMI 1640 medium and subcutaneously injected into posterior flank of nude mice (n = 6). Tumor size was measured using vernier caliper every 2 d when they were visible, and tumor volume was calculated according to the formula: volume = 0.5 × length × width^2.

Statistical analysis. Data were presented as mean ± SE of at least three independent experiments except specially indicated. Student's unpaired t-test was used for comparison of two independent groups. The correlations between miR-143 expression levels and clinicopathologic features or IHC staining scores of human CRC specimens were analyzed by Mann-Whitney test for two groups and Kruskall-Wallis test for three or more groups. Values were considered significantly different at $p < 0.05$.

Disclosure of Potential Conflicts of Interest

No potential conflicts of interest were disclosed.

Acknowlegements

This work was supported in part by National Natural Science Foundation of China (81071642, 30871296), Research and Innovation Project for College Graduates of Jiangsu Province, China (CXLX12_0550) and by National Cancer Institute, National Institutes of Health (R01CA109460).

Author Contributions

Xu Qian, Jing Yu, Jun He, Ling-Zhi Liu: study design, acquisition of data, analysis and interpretation of data, and manuscript preparation; Yu Yin, Lin Wang, Qi Li, Lou-Qian Zhang, Chong-Yong Li, Zhu-Mei Shi, Qing Xu, Wei Li: acquisition of data; Bing-Hua Jiang: study design, data interpretation, and manuscript preparation.

Supplemental Materials

Supplemental materials may be found here:
www.landesbioscience.com/journals/cc/article/24477

References

1. Parkin DM, Bray F, Ferlay J, Pisani P. Global cancer statistics, 2002. CA Cancer J Clin 2005; 55:74-108; PMID:15761078; http://dx.doi.org/10.3322/canjclin.55.2.74
2. Walsh JM, Terdiman JP. Colorectal cancer screening: scientific review. JAMA 2003; 289:1288-96; PMID:12633191; http://dx.doi.org/10.1001/jama.289.10.1288
3. Cunningham D, Atkin W, Lenz HJ, Lynch HT, Minsky B, Nordlinger B, et al. Colorectal cancer. Lancet 2010; 375:1030-47; PMID:20304247; http://dx.doi.org/10.1016/S0140-6736(10)60353-4
4. Han Y, Chen J, Zhao X, Liang C, Wang Y, Sun L, et al. MicroRNA expression signatures of bladder cancer revealed by deep sequencing. PLoS ONE 2011; 6:e18286; PMID:21464941; http://dx.doi.org/10.1371/journal.pone.0018286
5. Bartel DP. MicroRNAs: target recognition and regulatory functions. Cell 2009; 136:215-33; PMID:19167326; http://dx.doi.org/10.1016/j.cell.2009.01.002
6. Hermeking H. p53 enters the microRNA world. Cancer Cell 2007; 12:414-8; PMID:17996645; http://dx.doi.org/10.1016/j.ccr.2007.10.028
7. Volinia S, Calin GA, Liu CG, Ambs S, Cimmino A, Petrocca F, et al. A microRNA expression signature of human solid tumors defines cancer gene targets. Proc Natl Acad Sci USA 2006; 103:2257-61; PMID:16461460; http://dx.doi.org/10.1073/pnas.0510565103
8. Lichter P. All you need is a Mir-acle: the role of nontranslated RNAs in the suppression of B cell chronic lymphocytic leukemia. Cancer Cell 2010; 17:3-4; PMID:20129242; http://dx.doi.org/10.1016/j.ccr.2009.12.029
9. Lawrie CH, Gal S, Dunlop HM, Pushkaran B, Liggins AP, Pulford K, et al. Detection of elevated levels of tumour-associated microRNAs in serum of patients with diffuse large B-cell lymphoma. Br J Haematol 2008; 141:672-5; PMID:18318758; http://dx.doi.org/10.1111/j.1365-2141.2008.07077.x
10. Mitchell PS, Parkin RK, Kroh EM, Fritz BR, Wyman SK, Pogosova-Agadjanyan EL, et al. Circulating microRNAs as stable blood-based markers for cancer detection. Proc Natl Acad Sci USA 2008; 105:10513-8; PMID:18663219; http://dx.doi.org/10.1073/pnas.0804549105
11. Chen X, Ba Y, Ma L, Cai X, Yin Y, Wang K, et al. Characterization of microRNAs in serum: a novel class of biomarkers for diagnosis of cancer and other diseases. Cell Res 2008; 18:997-1006; PMID:18766170; http://dx.doi.org/10.1038/cr.2008.282
12. Taylor DD, Gercel-Taylor C. MicroRNA signatures of tumor-derived exosomes as diagnostic biomarkers of ovarian cancer. Gynecol Oncol 2008; 110:13-21; PMID:18589210; http://dx.doi.org/10.1016/j.ygyno.2008.04.033
13. Ahmed FE, Amed NC, Vos PW, Bonnerup C, Atkins JN, Casey M, et al. Diagnostic microRNA markers to screen for sporadic human colon cancer in blood. Cancer Genomics Proteomics 2012; 9:179-92; PMID:22798503
14. Ng EK, Chong WW, Jin H, Lam EK, Shin VY, Yu J, et al. Differential expression of microRNAs in plasma of patients with colorectal cancer: a potential marker for colorectal cancer screening. Gut 2009; 58:1375-81; PMID:19201770; http://dx.doi.org/10.1136/gut.2008.167817
15. Bihrer V, Waidmann O, Friedrich-Rust M, Forestier N, Susser S, Haupenthal J, et al. Serum microRNA-21 as marker for necroinflammation in hepatitis C patients with and without hepatocellular carcinoma. PLoS ONE 2011; 6:e26971; PMID:22066022; http://dx.doi.org/10.1371/journal.pone.0026971
16. Morimura R, Komatsu S, Ichikawa D, Takeshita H, Tsujiura M, Nagata H, et al. Novel diagnostic value of circulating miR-18a in plasma of patients with pancreatic cancer. Br J Cancer 2011; 105:1733-40; PMID:22045190; http://dx.doi.org/10.1038/bjc.2011.453
17. Liu J, Gao J, Du Y, Li Z, Ren Y, Gu J, et al. Combination of plasma microRNAs with serum CA19-9 for early detection of pancreatic cancer. Int J Cancer 2012; 131:683-91; PMID:21913185
18. Qu H, Xu W, Huang Y, Yang S. Circulating miRNAs: promising biomarkers of human cancer. Asian Pac J Cancer Prev 2011; 12:1117-25; PMID:21875254
19. Heegaard NH, Schetter AJ, Welsh JA, Yoneda M, Bowman ED, Harris CC. Circulating microRNA expression profiles in early stage non-small cell lung cancer. Int J Cancer 2012; 130:1378-86; PMID:21544802
20. Kosaka N, Iguchi H, Ochiya T. Circulating microRNA in body fluid: a new potential biomarker for cancer diagnosis and prognosis. Cancer Sci 2010; 101:2087-92; PMID:20624164; http://dx.doi.org/10.1111/j.1349-7006.2010.01650.x
21. Hu Z, Chen X, Zhao Y, Tian T, Jin G, Shu Y, et al. Serum microRNA signatures identified in a genome-wide serum microRNA expression profiling predict survival of non-small-cell lung cancer. J Clin Oncol 2010; 28:1721-6; PMID:20194856; http://dx.doi.org/10.1200/JCO.2009.24.9342
22. Dong X, Javle M, Hess KR, Shroff R, Abbruzzese JL, Li D. Insulin-like growth factor axis gene polymorphisms and clinical outcomes in pancreatic cancer. Gastroenterology 2010; 139(73 e1-3):464-73, e1-3; PMID:20416304; http://dx.doi.org/10.1053/j.gastro.2010.04.042
23. La Rocca G, Badin M, Shi B, Xu SQ, Deangelis T, Sepp-Lorenzinoi L, et al. Mechanism of growth inhibition by MicroRNA 145: the role of the IGF-I receptor signaling pathway. J Cell Physiol 2009; 220:485-91; PMID:19391107; http://dx.doi.org/10.1002/jcp.21796
24. Kong KL, Kwong DL, Chan TH, Law SY, Chen L, Li Y, et al. MicroRNA-375 inhibits tumour growth and metastasis in oesophageal squamous cell carcinoma through repressing insulin-like growth factor 1 receptor. Gut 2012; 61:33-42; PMID:21813472; http://dx.doi.org/10.1136/gutjnl-2011-300178
25. Jiang L, Liu X, Chen Z, Jin Y, Heidbreder CE, Kolokythas A, et al. MicroRNA-7 targets IGF1R (insulin-like growth factor 1 receptor) in tongue squamous cell carcinoma cells. Biochem J 2010; 432:199-205; PMID:20819078; http://dx.doi.org/10.1042/BJ20100859
26. Flanigan SA, Pitts TM, Eckhardt SG, Tentler JJ, Tan AC, Thorburn A, et al. The insulin-like growth factor I receptor/insulin receptor tyrosine kinase inhibitor PQIP exhibits enhanced antitumor effects in combination with chemotherapy against colorectal cancer models. Clin Cancer Res 2010; 16:5436-46; PMID:20943761; http://dx.doi.org/10.1158/1078-0432.CCR-10-2054
27. Zhang C, Wang J, Gu H, Zhu D, Li Y, Zhu P, et al. Capecitabine plus oxaliplatin compared with 5-fluorouracil plus oxaliplatin in metastatic colorectal cancer: Meta-analysis of randomized controlled trials. Oncol Lett 2012; 3:831-8; PMID:22741002
28. Lee RC, Feinbaum RL, Ambros V. The C. elegans heterochronic gene lin-4 encodes small RNAs with antisense complementarity to lin-14. Cell 1993; 75:843-54; PMID:8252621; http://dx.doi.org/10.1016/0092-8674(93)90529-Y
29. Xia H, Cheung WK, Ng SS, Jiang X, Jiang S, Sze J, et al. Loss of brain-enriched miR-124 microRNA enhances stem-like traits and invasiveness of glioma cells. J Biol Chem 2012; 287:9962-71; PMID:22253443; http://dx.doi.org/10.1074/jbc.M111.332627
30. Xia H, Ooi LL, Hui KM. MiR-214 targets β-catenin pathway to suppress invasion, stem-like traits and recurrence of human hepatocellular carcinoma. PLoS ONE 2012; 7:e44206; PMID:22962603; http://dx.doi.org/10.1371/journal.pone.0044206
31. Noman MZ, Buart S, Romero P, Ketari S, Janji B, Mari B, et al. Hypoxia-inducible miR-210 regulates the susceptibility of tumor cells to lysis by cytotoxic T cells. Cancer Res 2012; 72:4629-41; PMID:22962263; http://dx.doi.org/10.1158/0008-5472.CAN-12-1383
32. Fang R, Xiao T, Fang Z, Sun Y, Li F, Gao Y, et al. MicroRNA-143 (miR-143) regulates cancer glycolysis via targeting hexokinase 2 gene. J Biol Chem 2012; 287:23227-35; PMID:22593586; http://dx.doi.org/10.1074/jbc.M112.373084
33. Kent OA, Fox-Talbot K, Halushka MK. RREB1 repressed miR-143/145 modulates KRAS signaling through downregulation of multiple targets. Oncogene 2012; Epub Ahead of Print; PMID:22751122; http://dx.doi.org/10.1038/onc.2012.266
34. Gregersen LH, Jacobsen A, Frankel LB, Wen J, Krogh A, Lund AH. MicroRNA-143 down-regulates Hexokinase 2 in colon cancer cells. BMC Cancer 2012; 12:232; PMID:22691140; http://dx.doi.org/10.1186/1471-2407-12-232
35. Shi ZM, Wang J, Yan Z, You YP, Li CY, Qian X, et al. MiR-128 inhibits tumor growth and angiogenesis by targeting p70S6K1. PLoS ONE 2012; 7:e32709; PMID:22442669; http://dx.doi.org/10.1371/journal.pone.0032709
36. Pan J, Fauzee NJ, Wang YL, Sheng YT, Tang Y, Wang JQ, et al. Effect of silencing PARG in human colon carcinoma LoVo cells on the ability of HUVEC migration and proliferation. Cancer Gene Ther 2012; 19:715-22; PMID:22918473; http://dx.doi.org/10.1038/cgt.2012.48
37. Hart LS, Dolloff NG, Dicker DT, Koumenis C, Christensen JG, Grimberg A, et al. Human colon cancer stem cells are enriched by insulin-like growth factor-1 and are sensitive to figitumumab. Cell Cycle 2011; 10:2331-8; PMID:21720213; http://dx.doi.org/10.4161/cc.10.14.16418
38. Zhao D, Bakirtzi K, Zhan Y, Zeng H, Koon HW, Pothoulakis C. Insulin-like growth factor-1 receptor transactivation modulates the inflammatory and proliferative responses of neurotensin in human colonic epithelial cells. J Biol Chem 2011; 286:6092-9; PMID:21212273; http://dx.doi.org/10.1074/jbc.M110.192534
39. Fang J, Zhou Q, Liu LZ, Xia C, Hu X, Shi X, et al. Apigenin inhibits tumor angiogenesis through decreasing HIF-1alpha and VEGF expression. Carcinogenesis 2007; 28:858-64; PMID:17071632; http://dx.doi.org/10.1093/carcin/bgl205
40. Yuen JS, Akkaya E, Wang Y, Takiguchi M, Peak S, Sullivan M, et al. Validation of the type 1 insulin-like growth factor receptor as a therapeutic target in renal cancer. Mol Cancer Ther 2009; 8:1448-59; PMID:19509240; http://dx.doi.org/10.1158/1535-7163.MCT-09-0101
41. Poulaki V, Mitsiades CS, McMullan C, Sykoutri D, Fanourakis G, Kotoula V, et al. Regulation of vascular endothelial growth factor expression by insulin-like growth factor I in thyroid carcinomas. J Clin Endocrinol Metab 2003; 88:5392-8; PMID:14602779; http://dx.doi.org/10.1210/jc.2003-030389
42. Patel BB, Gupta D, Elliott AA, Sengupta V, Yu Y, Majumdar AP. Curcumin targets FOLFOX-surviving colon cancer cells via inhibition of EGFRs and IGF-1R. Anticancer Res 2010; 30:319-25; PMID:20332435
43. Patel BB, Sengupta R, Qazi S, Vachhani H, Yu Y, Rishi AK, et al. Curcumin enhances the effects of 5-fluorouracil and oxaliplatin in mediating growth inhibition of colon cancer cells by modulating EGFR and IGF-1R. Int J Cancer 2008; 122:267-73; PMID:17918158; http://dx.doi.org/10.1002/ijc.23097

44. Neugut AI, Becker DJ, Insel BJ, Hershman DL. Uptake of oxaliplatin and bevacizumab for treatment of node-positive and metastatic colon cancer. J Oncol Pract 2012; 8:156-63; PMID:22942809; http://dx.doi.org/10.1200/JOP.2011.000371
45. Kroh EM, Parkin RK, Mitchell PS, Tewari M. Analysis of circulating microRNA biomarkers in plasma and serum using quantitative reverse transcription-PCR (qRT-PCR). Methods 2010; 50:298-301; PMID:20146939; http://dx.doi.org/10.1016/j.ymeth.2010.01.032
46. Valeri N, Gasparini P, Braconi C, Paone A, Lovat F, Fabbri M, et al. MicroRNA-21 induces resistance to 5-fluorouracil by down-regulating human DNA MutS homolog 2 (hMSH2). Proc Natl Acad Sci USA 2010; 107:21098-103; PMID:21078976; http://dx.doi.org/10.1073/pnas.1015541107
47. Chen C, Ridzon DA, Broomer AJ, Zhou Z, Lee DH, Nguyen JT, et al. Real-time quantification of microRNAs by stem-loop RT-PCR. Nucleic Acids Res 2005; 33:e179; PMID:16314309; http://dx.doi.org/10.1093/nar/gni178
48. Wang X. A PCR-based platform for microRNA expression profiling studies. RNA 2009; 15:716-23; PMID:19218553; http://dx.doi.org/10.1261/rna.1460509
49. Jing Y, Liu LZ, Jiang Y, Zhu Y, Guo NL, Barnett J, et al. Cadmium increases HIF-1 and VEGF expression through ROS, ERK, and AKT signaling pathways and induces malignant transformation of human bronchial epithelial cells. Toxicol Sci 2012; 125:10-9; PMID:21984483; http://dx.doi.org/10.1093/toxsci/kfr256
50. Xu Q, Jiang Y, Yin Y, Li Q, He J, Jing Y, et al. A regulatory circuit of miR-148a/152 and DNMT1 in modulating cell transformation and tumor angiogenesis through IGF-IR and IRS1. J Mol Cell Biol 2013; 5:3-13; PMID:22935141
51. Zhang C, Hao L, Wang L, Xiao Y, Ge H, Zhu Z, et al. Elevated IGFIR expression regulating VEGF and VEGF-C predicts lymph node metastasis in human colorectal cancer. BMC Cancer 2010; 10:184; PMID:20459642; http://dx.doi.org/10.1186/1471-2407-10-184